

Constitutive Damage Modeling of Concrete in Compression with Dilatation

Chhabiraj Ghimire , Kamal Bahadur Thapa,

Pokhara University, Orchid Id: <https://orcid.org/0009-0004-0990-9074>

Abstract

Commencing with "In recent years," the abstract encapsulates the essence of advancements in concrete structure analysis and design. It highlights the shift from traditional methods to more sophisticated numerical analysis techniques, particularly focusing on the development of an anisotropic damage model for concrete within the framework of the internal variable theory of thermodynamics. This model intricately considers the influence of microcracks and microvoids on the material's behavior, offering insights into anisotropic damage and changes in elastic properties. Validated against experimental data and programmed in FORTRAN, the model emerges as a powerful tool for comprehensive structural analysis and design, empowering engineers with a nuanced understanding of concrete behavior under varying loading conditions.

Keywords:concrete structures, nonlinear analysis, anisotropic damage model, internal variable theory, damage mechanics, strain space formulation, FORTRAN programming, experimental validation.

1. Introduction

Concrete, a versatile and indispensable construction material, owes its widespread use to its remarkable properties: high compressive strength, fire resistance, and durability in harsh environments. However, its behavior under varying loads, especially plain concrete, exhibits complexity due to its non-isotropic nature and heterogeneous composition. The response of concrete to external forces is governed by the growth and nucleation of microcracks, leading to nonlinear stress-strain behavior. Traditional analytical methods have been supplemented by modern tools like finite element analysis, necessitating the development of realistic constitutive models. Continuum damage mechanics has emerged as a promising approach, providing a framework to describe concrete's behavior at both macroscopic and microscopic levels. Within this framework, microstructural degradation leads to reduced material stiffness, characterized by the propagation and coalescence of microcracks. Continuum damage mechanics models, typically formulated within a thermodynamic framework, offer insights into concrete's strain-softening response. In our investigation, we focus on plain concrete's stress-strain behavior under compressive loading, considering dilatation resulting from microcrack formation. Initially isotropic, concrete becomes anisotropic due to the presence of microcracks. The strain-based formulation within continuum damage mechanics proves advantageous over stress-based formulations, providing clarity in defining loading criteria and capturing strain softening behavior accurately. By delving into the realm of continuum damage mechanics, we aim to enhance our understanding of concrete behavior and pave the way for more accurate and reliable structural design practices.

2. Literature review

2.1 Uniaxial Compression

This section provides a foundational overview of the mechanical attributes of concrete, laying the groundwork for the comprehensive examination of constitutive modeling in subsequent sections. While macroscopic behavior is briefly touched upon, readers are encouraged to consult authoritative sources for detailed insights. Concrete is herein regarded as a continuum material with initial isotropic properties. Noteworthy is the exclusion of factors such as water-cement ratio, aggregate morphology, and cement composition, despite their known influence on mechanical performance. Concrete exhibits pronounced nonlinear characteristics in both

tension and compression. Specifically, in uniaxial compression, a distinct progression of stages is typically observed:

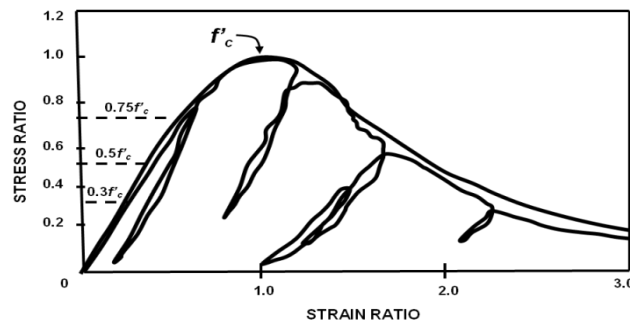


Figure:3.1 Stress-strain behavior of concrete under monotonic and cyclic compressive loading (Bhan and Hsu, 1988)

In uniaxial compression tests, concrete undergoes distinct stages of mechanical behavior, each characterized by specific stress-strain responses. Initially, up to approximately 30% of its maximum compressive strength (f_c), concrete behaves linearly elastically, with micro-cracks remaining inactive. However, beyond this threshold, cracking initiates, marking the onset of nonlinear behavior. Between 30% and 50% of f_c , stress concentrations at crack tips lead to stable propagation of bond cracks, while mortar cracks remain largely unaffected. Within this range, crack growth remains stable under constant stress conditions. As the stress level increases further, ranging from 50% to 75% of f_c , mortar cracks propagate steadily, with some new bond cracks forming gradually. Under constant load, cracks continue to grow until reaching their final lengths, exhibiting a stable pattern of crack propagation. Beyond approximately 75% of f_c , however, cracks widen and propagate more rapidly, indicative of unstable crack propagation. The internal energy now surpasses the energy needed for crack release, potentially culminating in complete failure of the concrete specimen, even under constant loading conditions. It's notable that concrete displays significant strain softening beyond peak stress, resulting in deformation localization and a lack of a unique stress-strain relationship. This strain softening behavior, observed in both tension and compression, underscores the complex nature of concrete's mechanical response and poses challenges in accurately characterizing its behavior.

2.2 Volume expansion under compressive loading:

As a concrete specimen undergoes increasing uniaxial compression, its apparent Poisson's ratio deviates significantly from its initially established elastic value. This deviation becomes pronounced beyond a critical stress level, typically between 75% to 90% of the ultimate uniaxial compressive stress. At this point, known as the initiation stress, the concrete's volume begins to increase rather than continuing to decrease, reflecting its composite nature. This inelastic behavior has been observed by researchers such as Domingo Sfer et al. and Shah and Chandra (1968), and it signifies a notable shift in the mechanical response of the material.

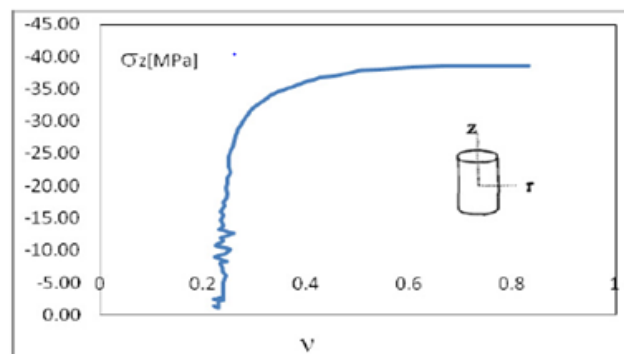


Figure: 3.2 Poisson's ratio vs stress, under uniaxial compression (D. Sfer et al)

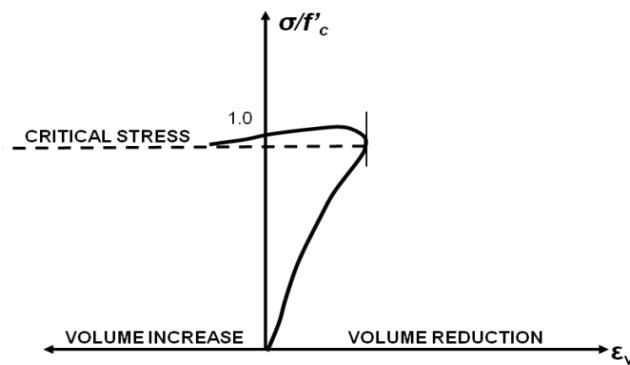


Figure: 3.3 Typical stress-volumetric strain curve for concrete in uniaxial compression (data from Kupfer et al., 1969)

Cracks in concrete are not strictly parallel to the compressive loading axis; rather, they are inclined at certain angles due to irregularities in aggregate shapes. These inclined cracks, known as bond cracks, generate shear stress components within the material. These shear stresses induce shear sliding and surface separation along the crack faces, ultimately compromising the aggregate-mortar interface. As loading continues, cracks propagate along preferred cleavage planes, eventually aligning parallel to the loading axis.

2.3 Biaxial Compression

Concrete structural members, such as beams and shells, often experience biaxial stress states due to complex external loads, necessitating a thorough understanding of concrete behavior under such conditions. Over the past century, numerous experiments have been conducted to elucidate concrete's stress-strain relationships in biaxial stress paths. However, most research has focused on biaxial compression, with limited data available for biaxial tension and combined compression-tension scenarios. Experimental findings by Kupfer et al. (1969) suggest that concrete exhibits similar strengths under uniaxial and biaxial tensile stress paths, independent of stress ratio. However, in combined compression and tension, increased tensile stress reduces the compressive strength of concrete. In biaxial compression tests, concrete specimens undergo increasing compressive stresses in two perpendicular directions, while the third direction remains stress-free. Results indicate that the biaxial strength of concrete varies with stress ratio, peaking at a ratio of 0.5. At this ratio, the maximum strength is approximately 27% higher than the uniaxial compressive strength (f_c) of concrete. Strength and ductility both increase to some extent under biaxial compression stress states, with volume expansion occurring near the peak load.

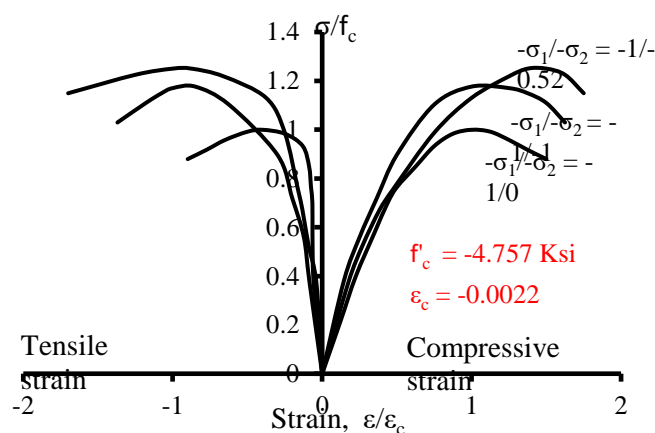


Figure: 3.4 Stress- strain relationship of concrete under biaxial compression (Kupfer et al., 1969)

2.4 Triaxial Compression

Behaviour of concrete in triaxial compression tests differs significantly from that observed in uniaxial and two-way compression. In triaxial compression, concrete undergoes increasing axial compressive load under constant confining pressure until failure. Three distinct features are observed based on the level of confinement: quasi-brittle, plastic softening, and plastic hardening. Under high confining pressure, concrete exhibits enhanced strength and ductility, with failure occurring due to crushing rather than splitting. Concrete under pure hydrostatic pressure behaves differently from triaxial compression. Crack formation is negligible under hydrostatic compression, leading to no damage assumed to occur due to the passive micro-crack field. Shear stress governs compaction behavior, with concrete compacting more effectively under shear stress compared to hydrostatic pressure. This phenomenon is illustrated by the pressure-volumetric strain curve, where pressure required for compaction is lower under shear stress.

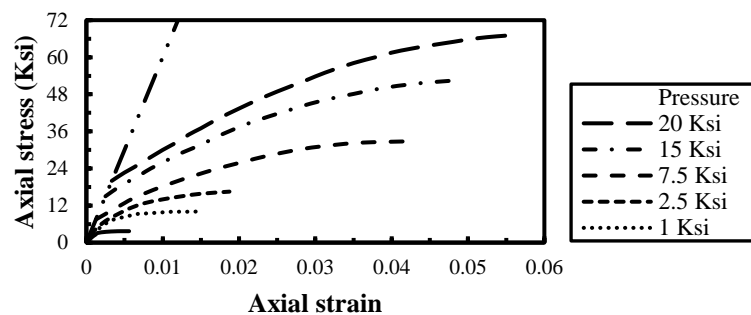


Figure: 3.5 Stress-strain curves of concrete in triaxial compression (Balmer, 1949)

2.5 Constitutive Modeling of Concrete

Numerous contributions have been made in developing constitutive models to understand the complex behavior of concrete. Karsan and Jirsa (1969) proposed an empirical formula correlating residual plastic strain with the onset of unloading. Kupfer et al. (1969) studied failure in both uniaxial and biaxial compression, finding similar strengths in tension but reduced compressive strength under combined loading. Ortiz (1985) proposed a theory of distributed damage and mixture theories for concrete inelasticity. Gopalaratnam and Shah (1985) developed a method for tension load-deformation behavior characterization. Yazdani and Karnawat (1996) incorporated damage and inelastic flow in a single-flow surface model. Yazdani and Schreyer (1988, 2003) developed an anisotropic damage model for concrete, extended to fatigue damage. Shang and Song (2006) investigated plain concrete behavior under biaxial compression after freeze-thaw cycles. Khan et al. (2007) proposed an effective compliance matrix concept to describe concrete damage. Thapa and Yazdani (2013) formulated a model within continuum thermodynamics to capture concrete inelasticity features.

3.0 General Formulation

3.1 General formulation for uniaxial compression:

Regarding the behaviour that is independent of rate and minute deformations, the internal energy per unit volume, U , can be taken as;

$$U = U(\varepsilon, s, k) \quad (1)$$

Where, ε , s and k represent the internal variable parameter, the strain tensor, and the local entropy per unit volume, respectively. The parameter 'k' defines the damage in the material caused by cracks and micro-cracks. Two types of thermodynamic potentials as shown below can be obtained with the application of Legendre Transformation:

$$A(\varepsilon, \theta, k) = U(\varepsilon, s, k) - \theta s \quad (2)$$

$$G(\sigma, \theta, k) = \sigma : \varepsilon - A(\varepsilon, \theta, k) \quad (3)$$

In this case, A and G stand for the respective Gibbs Free Energy (GFE) and Helmholtz Free Energy (HFE) per unit volume. σ is the Cauchy stress tensor and θ is absolute temperature. In this theory, it is assumed that, the parameter k alters the elastic properties of brittle materials resulting into elastic and inelastic deformations caused by the process of damage only. The development and growth of cracks and micro-cracks affects the elastic properties due to which gradual reduction of stiffness of the material takes place (Ortiz 1985, Yazdani and Shreyer 2003, Thapa and Yazdani 2013, 2014, Bhandari and Thapa 2013, Shrestha and Thapa 2015, Horii and Nemat-Nasser 1983)

Regarding the behaviour that is independent of rate and minute deformations, the rate form of the Helmholtz Free Energy(HFE) per unit volume, $A(\epsilon, \theta, k)$ is given by:

$$\dot{A} = \frac{\partial A}{\partial \epsilon} : \dot{\epsilon} + \frac{\partial A}{\partial \theta} \dot{\theta} + \frac{\partial A}{\partial k} \dot{k} \quad (4)$$

Equation (4) is used with the Clausius-Duhem inequality of the form:

$$-\dot{A} - \dot{\theta} s + \sigma : \dot{\epsilon} - \frac{q \Delta \theta}{\theta} \geq 0 \quad (5)$$

To obtain

$$ds = \left(\sigma - \frac{\partial A}{\partial \epsilon} \right) : \dot{\epsilon} - \left(s + \frac{\partial A}{\partial \theta} \right) \dot{\theta} - \frac{\partial A}{\partial k} \dot{k} - \frac{q \Delta \theta}{\theta} \geq 0 \quad (6)$$

Where, d_s is the dissipation rate, q denotes the heat flux vector. Tensor contraction is represented by the colon (:). The rate form of the variable is denoted by the superdot. Assuming that unloading is an elastic process, the usual thermodynamic arguments (Coleman and Gurtin 1967) yield the following three essential results:

(i) The Helmholtz Free Energy acts as a potential for entropy

$$s = - \frac{\partial A}{\partial \theta} \quad (7)$$

(ii) The stress tensor, which means the HFE is the potential for the stress tensor for strain-space formulation and

$$\frac{\partial A}{\partial \epsilon} = \sigma \quad (8)$$

(iii) The expression for the dissipation inequality is obtained as

$$ds = - \frac{\partial A}{\partial k} \dot{k} - \frac{q \Delta \theta}{\theta} \geq 0 \quad (9)$$

For isothermal process, $\Delta \theta = 0$, and hence equation (9) reduces to

$$ds = - \frac{\partial A}{\partial k} \dot{k} \geq 0 \quad (10)$$

Where $\frac{\partial A}{\partial k}$ signifies the thermodynamic force associated with the conjugate effective flux \dot{k} . In all procedures that are accepted, the disparity that is shown by equation (10) must be satisfied.

From equation (8), one can express

$$\frac{\partial A}{\partial \epsilon} = \sigma = E(k) : \epsilon \quad (11)$$

where $E(k)$, which is dependent on the degree of microcracking, is the fourth order current stiffness tensor. According to several studies, the fourth order elastic compliance tensor evolves with damage rather than being constant during the damage process (Ortiz 1985, Thapa and Yazdani 2013, 2014). The material stiffness tensor's components can capture induced anisotropic effects due to the dependence of $E(k)$ on the damage parameter. Adopting the concept from Thapa and Yazdani (2013), the fourth order stiffness tensor $E(k)$ is decomposed as follows:

$$E(k) = E^o + E^D(k) \quad (12)$$

Where, E^0 is the elastic stiffness tensor for an uncracked concrete and $E^D(k)$ corresponds to the induced degraded stiffness due to microcracking (damage).

Assuming that the inelasticity is caused only due to damage, the decoupled theory states that

$$A(\varepsilon, k) = A^e(\varepsilon, k) + A^D(\varepsilon, k) + A^i(\varepsilon, k) \quad (13.1)$$

Where, A^e , A^D and A^i are related to the elastic, elastic damage and inelastic damage process. These different processes can be expressed as follows:

$$A^e = \frac{1}{2} \varepsilon : E^0 : \varepsilon \quad (13.2)$$

$$A^D = \frac{1}{2} \varepsilon : E^D(k) : \varepsilon \quad (13.3)$$

$$A^i = \varepsilon : \sigma^i(k) \quad (13.4)$$

Where E^0 and $E^D(k)$ are the fourth order stiffness tensor for uncracked material and degraded stiffness tensor due to damage process. σ^i is the inelastic (relaxation) stress tensor.

Combining equation ($\sigma = \frac{\partial A}{\partial \varepsilon}$), (12) and (13) yields the following expression for the total stress tensor:

$$\sigma = \frac{\partial A}{\partial \varepsilon} = E^0 : \varepsilon + E^D(k) : \varepsilon + \sigma^i = \sigma^e + \sigma^D + \sigma^i = E(k) : \varepsilon + \sigma^i(k) \quad (14)$$

Where, $E(k)$ is the stiffness tensor of secant elastodamage, which is connected to the internal energy by

$$E(k) = E^0 + E^D(k) = \frac{\partial^2 U}{\partial \varepsilon \partial \varepsilon} \quad (15)$$

Where, σ^e , σ^D and σ^i are the components of the total stress tensor that are related to the decomposition of the total strain tensor, namely the elastic, damage, and inelastic damage parts. The relationship between the inelastic stress is

$$\sigma^i = -E(k) : \varepsilon^i \quad (16.1)$$

Since elastic unloading is predicated on the inelastic components being fixed.

From the dissipative inequalities equation ($-\frac{\partial A}{\partial k} \cdot \dot{k} \geq 0$) and equation (13), it follows that

$$-\frac{1}{2} \varepsilon : \dot{E}^D(k) : \varepsilon \geq 0 \quad (16.2)$$

$$-\varepsilon : \dot{\sigma}^i \geq 0 \quad (16.3)$$

Suppose the damage stiffness and inelastic stress tensors are described through the evolution equations:

$$\dot{E}^D(k) = -\dot{K}L(\varepsilon) \quad (17.1)$$

$$\dot{\sigma}^i = \dot{E}(k) : \varepsilon^i + E(k) : \dot{\varepsilon}^i \quad (17.2)$$

The inelastic strains in brittle materials like concrete are caused by inelastic micro fracturing process. During damage, process, the formation of a substantial crack tip process zone and crack surface misfits are the major sources of these inelastic deformations.

To address inelastic deformations in compressive mode of cracking, ε^- is considered as a proper strain tensor. The deviatoric part of ε^- is involved in the inelastic deformation process as the hydrostatic compression does not participate in this process. Let R^- and R^+ be the negative and positive cones of ε^{-d} respectively. The deviatoric part of ε^- represented by ε^{-d} is obtained as follows:

$$\varepsilon^{-d} = \varepsilon^- - \frac{\text{tr}(\varepsilon^-)}{3} \quad (18)$$

By definition of R^- and R^+ , one can express $\text{tr}(\varepsilon^{-d}) = 0$ leading to the condition

$$\text{tr}(R^-) + \text{tr}(R^+) = 0 \quad (19)$$

R^- and R^+ are null tensors under pure hydrostatic compression.

The experimental work of Resende and Martin (1984) showed that rock under uniaxial compression exhibits inelastic volumetric strain and dilation. These types of response features are also evident in frictional material like concrete. Concrete specimen loaded about the stress level of 75 to 90% of f_c , the lateral strain abruptly increases due to widening of the external cracks and the volume expansion (dilatation) takes place (Kupfer et al 1969; Wee et al 1996). Here f_c is defined as the uniaxial compressive strength of concrete. Shah and Chandra (1968) reported that the composite nature of concrete is the main reason for this inelastic behavior and volume expansion. The reversal of the stress-volumetric strain curve shown in Figure: 3.1 depict the dilatation behavior of frictional material such as concrete.

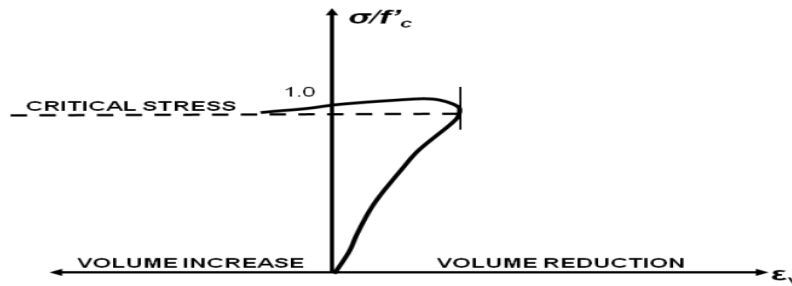


Figure: 3.1 Stress-volumetric strain curve as per Kupfer et al.

To capture this phenomenon of increase in volume and inelastic volumetric strain in concrete under compressive loading, it is necessary to create an evolution law for the inelastic strain tensor rate and included in the constitutive relation. As the volume expansion is observed in concrete, $\text{tr}(\dot{\varepsilon}^i)$ should be positive scalar (Yazdani and Schreyer, 1988). Guided by the Experimental work of Resende and Martin (1984) and Equation (19), the expression for rate of inelastic strain is formulated as follows:

$$\dot{\varepsilon}^i = \frac{E^0}{(E^0 - k)^2} \dot{k} (R^- + \alpha R^+) \quad (20)$$

Integrating of equation (20) yields

$$\varepsilon^i = \frac{E^0}{(E^0 - k)} k (R^- + \alpha R^+) \quad (21)$$

The scalar coefficient α is taken as greater than unity to capture inelastic strains. α is established using the common uniaxial compression tests on concrete. The inelastic volumetric strain is found to be null with value of $\alpha = 1$, and becomes analogous approach of Van Mises Plasticity theory applied to metals permanent deformations are not predicted by the model for purely hydrostatic compression.

The rate form of equation (4) is given by

$$\dot{\sigma} = \dot{E}(k) : \varepsilon + E(k) : \dot{\varepsilon} + \dot{\sigma}^i(k) = \dot{\sigma}^e + \dot{\sigma}^D + \dot{\sigma}^i \quad (22)$$

Where $\dot{\sigma}^e$ is the stress increment when the further growth of microcracks are prevented in the material, $\dot{\sigma}^D$ is the material's microcracks and cracks formed at a slower rate, which reduced the stress, and $\dot{\sigma}^i$ is the development of crack tip process zones and misfits and crack surfaces during damage process.

Again, integration of equation (14) with respect to ε yields

$$A(\varepsilon, k) = \frac{1}{2} \varepsilon : E(k) : \varepsilon + \sigma^i(k) : \varepsilon + A^i(k) \quad (23)$$

Where $A^i(k)$ is the inelastic component of the HFE associated with the surface energy of microcracks (Chaboche 1992 and 1993).

The formulation is mainly based on the concept of active and passive microcracks introduced by Ortiz (1985) and used by Thapa and Yazdani (2013). The nature of the damage is progressive and makes the concrete more compliant resulting into the reduction of elastic stiffness and development of inelastic deformation. Although concrete in this work is assumed as an isotropic material comprised of single phase continuum, the development of microcracks makes it highly anisotropic. The process of development of microcracks in the direction of applied loading is identified as active microcracking and there are two modes of active microcracking in concrete and they are mode I and mode II (Ortiz 1985, Yazdani and Karnawat 1996, Thapa and Yazdani 2013,2014). They are explained below:

Mode I:

It is also called splitting or cleavage mode of cracking. In this mode, opening of a planner crack takes place in the direction of tensile load refer Figure: 3.3. As the loading is reversed, the closing of the same microcracks takes place. This mode is symbolically expressed by the inequality $\varepsilon_I^d \geq 0$, where ε_I^d represents the strain due to crack opening in mode I. This means the total strain in the direction tensile loading increases due to mode I cracking.

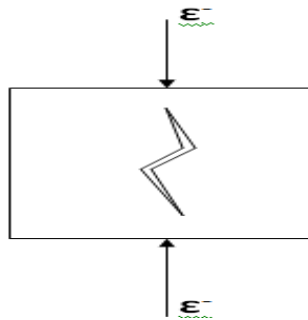


Figure : 3.2 Mode II cracking

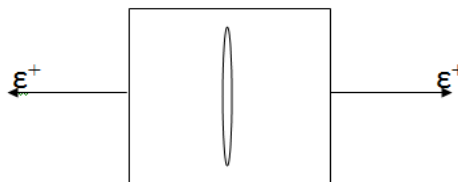


Figure: 3.3 Mode I cracking

Mode II

This refers to compressive mode of cracking; cracks extend in the direction compression loading. These cracks are not straight but follow tortuous path and leaves the possibility of crack opening in the lateral direction refer Figure : 3.2. These tortuous extended cracks lying in the average plane of compressive loading contribute to the decrease in the overall stiffness of the material. This compressive mode of microcracking opening is mathematically expressed as $\varepsilon_{II}^d \leq 0$.

Mode I damage contributes additional tensile strain due to crack opening in the direction of tensile loading, whereas mode II damage gives additional negative strain due to squeezing of the material in the direction of compressive loading and the opening of extended cracks in the lateral direction. Mode I always has positive eigenvalues of strain tensor stretching. Mode II damage always possesses negative as well as positive eigenvalues of strain tensors to ensure both squeezing of the material in the direction of compressive loading and cracks, opening in the lateral directions. The strain tensor which contains the positive eigenvalues is termed the positive cone, whereas the negative eigenvalues of strain tensor are regarded as the negative cone.

Figure : 3.2 shows the compressive mode of cracking in which only one crack is shown for simplification. The response tensor formulated is able to capture the behavior of concrete failure in uniaxial compression loading in which specimen fail by uniting numbers of cracks formed during loading.

Equation (10) presents an inequality that needs to be satisfied for all admissible processes. The substitution of Eqns (23) and (12) into Eqn (10) yield

$$ds = -\frac{1}{2} \varepsilon : \dot{E}^D : \varepsilon - \dot{\sigma}^i(k) : \varepsilon - \dot{A}^i(k) \geq 0 \quad (24)$$

Damage Surface

To proceed further, let the rate of the reduced stiffness tensor used in Eqn (24) be represented by the subsequent linear damage law that is independent of rate.

$$\dot{E}^D = -\dot{k}L(\varepsilon) \quad (25)$$

where, $L(\varepsilon)$ is a fourth-class reaction tensor which determines the path of the harm in the material. Substitution of Eqn (25) into Eqn (24) yields the dissipation as

$$d_s = \dot{k} \left(\frac{1}{2} \varepsilon : \dot{E}^D : \varepsilon + \dot{\sigma}^i(k) : \varepsilon + \dot{A}^i(k) \right) \geq 0 \quad (26)$$

Since Since damage is irreversible, $\dot{k} > 0$ by definition. K is the energy dissipation unit. Moreover, In the absence of any internal constraints, the coefficient of \dot{k} must be nonnegative, as stated by Ortiz (1985). Consequently, Eqn(26) can be written as

$$\left(\frac{1}{2} \varepsilon : \dot{E}^D : \varepsilon + \dot{\sigma}^i(k) : \varepsilon + \dot{A}^i(k) \right) \geq 0 \quad (27)$$

All that has to be done to push the right hand side of Eqn (27) to zero is to add a positive valued function, It is now possible to define the damage surface or harm potential. Let's assume that a positive function $G^2(\varepsilon, k)$, the damage surface ψ takes on the following form

$$\psi(\varepsilon, k) = \frac{1}{2} \varepsilon : L : \varepsilon + \dot{\sigma}^i(k) : \varepsilon - \frac{1}{2} p^2(\varepsilon, k) = 0 \quad (28.1)$$

$$\psi(\varepsilon, k) = \frac{1}{2} \varepsilon : L : \varepsilon + (\dot{E}(k) : \varepsilon^i + E(k) : \varepsilon^i) : \varepsilon - \frac{1}{2} p^2(\varepsilon, k) = 0 \quad (28.2)$$

Where,

$$p^2(\varepsilon, k) = 2(A_k^i + G^2(\varepsilon, k)) \quad (29)$$

The function $p^2(\varepsilon, k)$ is identified as the damage function. We further note that there is no need to individually identify A_k^i and G^2 functions as long as the damage function itself could be determined. Eqn (28.2) effectively completes the general formulation of the proposed model by using the normal Kuhn-Tucker loading-unloading criteria (i.e., $\dot{k} \geq 0$, $\psi \leq 0$ and $\dot{k}\psi = 0$). However, in order to completely define a certain substance, the details need to be sorted out. Specific expressions for the response tensor, L , and particular forms of the damage function, p would represent different damage models for this class of damage mechanics theories.

3.2 Development of proposed model for concrete in compression:

The damage model is proposed through the formulation of proper forms of the response tensors and the corresponding damage function. The response tensor should be capable of capturing the anisotropic nature of the damage in concrete. There are two cones in the strain tensor: positive and negative in order to achieve these. The matching negative and positive eigenvalues of the system are held by the positive and negative cones of the strain tensor as

$$\varepsilon = \varepsilon^+ + \varepsilon^- \quad (30)$$

where ε^+ represents the positive cone of the strain tensor and ε^- represents the negative cone of the strain

tensor. The formal mathematical procedure for decomposition of tensors is described in Ortiz (1985) and Ju (1989) and will not be repeated here.

At the same time, a large body of experimental tests on concrete in tension and compression has left researchers to identify two dominant and distinct crack patterns in concrete. The cleavage mode is one (or mode I) cracking due to tensile loads and the other one is the compression mode (or mode II) cracking (Horii and Nemat-Nasser 1983). Mode I or tensile mode solely represents the opening of cracks in the direction of tensile load, whereas Mode II represents the shear sliding of cracks along the crack lines which will lead to both the direction in which the cracks are extending of the compressive load and opening of cracks in the lateral direction. For small deformation, a possible way to include these two modes of damage is to decompose the rate of degraded stiffness tensor as follows:

$$\dot{E}^D(K) = \dot{E}_I^D(K) + \dot{E}_{II}^D(K) \quad (31)$$

where damage modes I and II are denoted by the subscripts I and II, respectively. Following Eqn (25), one obtains

$$\dot{E}_I^D(K) = -\dot{k}L_I \text{ and } \dot{E}_{II}^D(K) = -\dot{k}L_{II} \quad (32)$$

where L_I and L_{II} are fourth-order response tensors for damage in mode I and II respectively. Guided by the experimental results and observation for concrete materials in tension (Gopalaratnam and Shah 1985) where it is demonstrated that the majority of damage occurs in the direction of maximal strain, the response tensor, L_I , is proposed

$$L_I = \frac{(\varepsilon^+ \otimes \varepsilon^+)}{(\varepsilon^+ : \varepsilon^+)} \eta \quad (33) \quad \text{The parameter}$$

η is shown here to take into account the cumulative impact of harm brought on via tensile alterations connected to various directions, and is given by

$$\eta = 1 + \beta(1 + \phi_1) \left(1 - \frac{\lambda}{\text{tr } \varepsilon^+}\right) \quad (34)$$

Where, λ is the maximum eigenvalue of ε^+ , ϕ_1 is the minimum eigen value of ε and β is the material constant to be selected in light of the brittle material's characteristics. On the other hand, a combination of lateral fracture opening and crack extension in the direction of applied compressive loads results in mode II cracking. Consequently, the response tensors shown below can be used to create the entire response function for mode II damage:

$$L_{II} = w(L_{II}^d + L_{II}^h) \quad (35)$$

where w is a material property that explains how concrete behaves relative to other materials under tension and compression. The component L_{II}^h incorporates the damage due to opening of cracks in the lateral directions. The form for L_{II}^h as therefore proposed here

$$L_{II}^h = \frac{(\varepsilon^+ \otimes \varepsilon^+)}{(\varepsilon^+ : \varepsilon^+)} \eta \quad (36)$$

The experimental observation on brittle solid such as concrete has shown that no damage takes place under purely hydrostatic pressure. The response tensor L_{II}^d postulated to be:

$$L_{II}^d = \frac{(\tilde{\varepsilon} \otimes \tilde{\varepsilon})}{(\tilde{\varepsilon} : \tilde{\varepsilon})} \quad (37)$$

Here' $\tilde{\varepsilon} = \varepsilon^- - \delta i$, δ is The second order identity tensor is the greatest eigenvalue of ε^- and i . The replacement of response tensors with specific forms L_I and L_{II} from Eqns 15 through 19 into Eqn 9 results in the damage surface's ultimate form;

$$\begin{aligned} \psi(\varepsilon, k) &= \frac{1}{2} \varepsilon : \frac{(\varepsilon^+ \otimes \varepsilon^+)}{(\varepsilon^+ : \varepsilon^+)} : \varepsilon \eta H(\lambda_1) + \frac{1}{2} w H(-\lambda_2) \varepsilon : \left(\frac{(\tilde{\varepsilon} \otimes \tilde{\varepsilon})}{(\tilde{\varepsilon} : \tilde{\varepsilon})} + \frac{(\varepsilon^+ \otimes \varepsilon^+)}{(\varepsilon^+ : \varepsilon^+)} \eta \right) : \varepsilon + (\dot{E}(k) : \varepsilon^i + E(k) : \dot{\varepsilon}^i) : \varepsilon - \\ &\frac{1}{2} p^2(\varepsilon, k) = 0 \end{aligned} \quad (38)$$

where, $H(\cdot)$ signifies the Heaviside function, $\lambda_1 = \text{tr}(\sigma^+)$ and $\lambda_2 = \text{tr}(\sigma^-)$.

$$P(k) = \varepsilon_u \left(\frac{k}{E^0 - k} \right)^{\frac{1}{2}}$$

w = The material parameter that explains how strong concrete is in tension and compression.

ε^+ represents the positive cone of the strain tensor and ε^- symbolises the strain tensor's negative cone.

ε is strain tensor.

ε^i is inelastic strain tensor.

$\dot{\varepsilon}^i$ is rate of inelastic strain tensor.

$E(k)$ is fourth order stiffness tensor.

$\dot{E}(k)$ is rate of fourth order stiffness tensor.

4.0 Calculation, Results And Discussion

4.1 Calculation:

For the calculations purpose equations derived in previous chapter are used and computation is done in FORTRAN. Program codes (as shown in appendix) are developed and different values were obtained. In uniaxial compression, curve between axial and lateral strains (ε_1 and ε_2) – stress (σ) and volumetric strain (ε_v) – stress (σ). Curves obtained after computation of the model are compared with experimental results. Materials parameters taken for the calculations are as follows:

Parameters	Values
E^0	30768.7 MPa (4454.02 Ksi) (Young's modulus)
N	0.2 (Poisson's ratio)
ε_u	0.0003 (Strain corresponding to uniaxial tensile strength)
ε_c	0.0022 (Strain corresponding to uniaxial compressive strength)
β	0.75
W	0.0049
μ	0.15 (Plastic cracking coefficient)
f_t	2.6 MPa (0.38 Ksi) Uniaxial tensile strength of concrete
f_c	32.8 MPa (4.757 Ksi) Uniaxial compressive strength of concrete

4.2 Results:

Figure 4.1 shows the Damage function variation, $p(k)$, with the scalar damage parameter, k . The following figure shows that when there is no damage, k takes the value zero so that $p(k)$ is zero. As, k increases, $p(k)$ also increases and the limit is reached for when k approaches the initial value of Young's modulus.

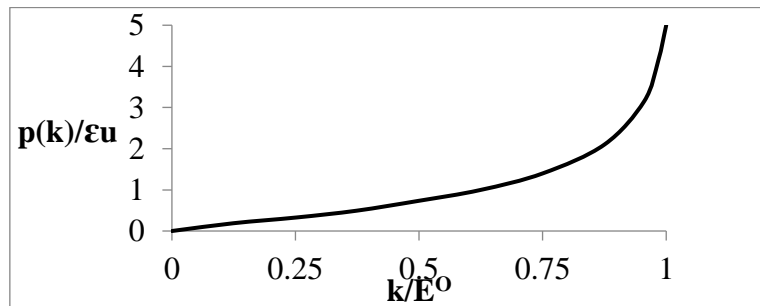


Figure: 4.1 Variation of damage function $p(k)$ with the damage parameter k

The theoretical curve of stress-volumetric strain is shown in Figure 4.2. The theoretical curve is compared utilising the Kupfer et al. (1969) data, and the agreement is seen to be satisfactory for strength and ductility. The results are normalized relative to the compressive strength in one dimension, f_c , and the corresponding strain, ϵ_c .

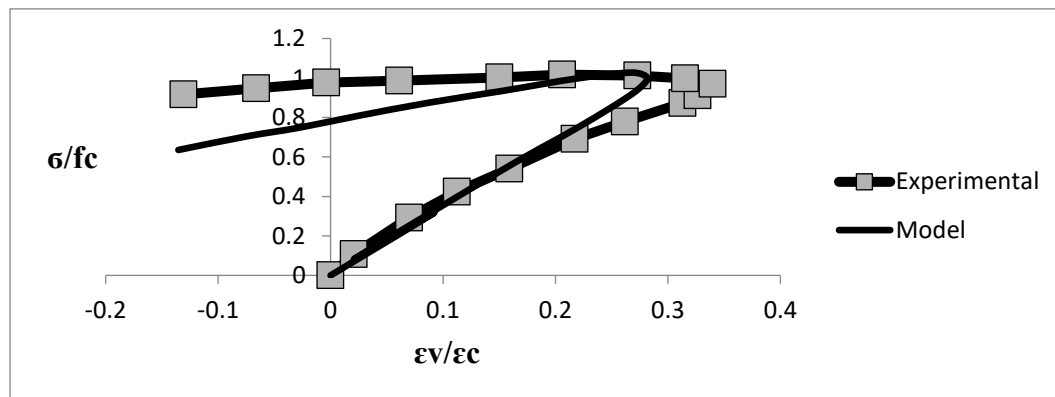


Figure: 4.2 Stress-Volumetric strain curve compared with experimental data of Kupfer et al. (1969)

The theoretical curve for uniaxial compression and proportional load path are shown in Figure: 4.3, where a graphic of Kupfer et al. (1969)'s experimental data average values is also included. The results are normalized relative to the uniaxial compressive strength, f_c , and the corresponding strain ϵ_c . For strength and ductility, there is a satisfactory agreement between the model and the experiment.

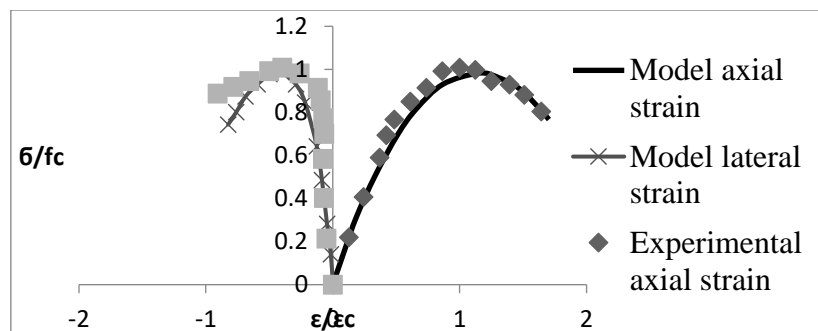


Figure: 4.3 Stress-strain curve of concrete compared with experimental data

4.3 Limitations of study

The Proposed model is casted within the following boundaries:

- The model considers only damage mechanics approach.
- Assumes initially material is isotropic and becomes anisotropic with the development of cracks.
- Concrete is considered as continuum and single phase material.
- Fatigue damage is not considered.
- Visco-elastic behavior of concrete is not considered.
- This model works only for uniaxial compression.

5.0 Conclusion And Recommendations

The stress-strain relationship elucidated by this model portrays a distinct non-linear trajectory. Initially, the curve exhibits linear behavior up to approximately 30% of the maximum compressive strength, after which it diverges onto a non-linear path. This transition marks a critical point where the inherent microstructure of concrete begins to undergo significant changes in response to increasing stress. As the stress intensifies, the concrete initially experiences a reduction in volume. However, beyond a critical stress threshold, a notable

phenomenon known as dilatancy occurs, where the volume of the concrete starts to increase rather than decrease. This intricate behavior underscores the composite nature of concrete and the complex interplay of its constituent materials under varying stress levels. The theoretical underpinning of this model is rooted in the Internal Variable Thermodynamic Theory, coupled with damage mechanics employing strain space formulation. Within this framework, the model introduces a novel concept of permanent deformation, which mirrors observations in various materials undergoing stress. Concrete, regarded here as a single-phase continuum material, begins as isotropic but gradually transitions to an anisotropic state as cracks propagate through its structure. While the model adeptly characterizes the mechanical response of concrete under uniaxial compression, it does not encompass the complexities of fatigue damage or viscoelastic behavior, which are pertinent in certain real-world scenarios. Comparative analysis with experimental data obtained from Kupfer et al. (1969) reveals a commendable alignment between the model predictions and empirical observations. Critical stress, uniaxial compressive strength, and corresponding strains demonstrate a satisfactory agreement between the model's outputs and experimental results. However, it's essential to recognize that variations in the experimental stress-strain curves can be attributed to diverse testing conditions. Factors such as specimen size, strain rate, machine stiffness, loading methodology, and measurement techniques exert significant influence, highlighting the need for comprehensive consideration of testing conditions in future iterations of the model.

5.2 Recommendation for the further study

Continued advancements and expansions of this model could explore its applicability in multiaxial compression scenarios, where concrete structures often encounter complex stress states. Integrating multiaxial compression into the model could provide valuable insights into concrete behavior under more realistic loading conditions encountered in practical engineering applications. Additionally, incorporating a combined damage-plasticity approach into the modeling framework could enhance its predictive capabilities by offering a comprehensive representation of the interplay between damage accumulation and plastic deformation, thereby providing a nuanced understanding of concrete's response to compressive loading. Furthermore, considering stress space formulation could offer valuable insights into the behavior of plain concrete under diverse stress conditions. Stress space formulations provide a systematic framework for analyzing material behavior across different stress states, enabling a more thorough characterization of concrete's mechanical response. By incorporating stress space formulations, the model could capture the complex stress-strain relationships exhibited by concrete under varying loading scenarios, thereby improving its accuracy and predictive capabilities. Moreover, extending the model to address fatigue-related phenomena would be essential for applications in which concrete structures undergo cyclic loading over extended periods. Fatigue can significantly influence the structural integrity and durability of concrete elements, making it a critical consideration in engineering design and analysis. By integrating fatigue effects into the model, engineers could better evaluate the long-term performance of concrete structures and implement appropriate design strategies to mitigate fatigue-related failures. Overall, these potential extensions offer promising avenues for advancing the understanding and modeling of plain concrete behavior under compressive loading, thereby enhancing the reliability and effectiveness of structural designs in practice.